

DEPARTMENT OF ENGINEERING RESEARCH
UNIVERSITY OF MICHIGAN
ANN ARBOR

QUARTERLY PROGRESS REPORT

By
Keith A. Pierce
Leo Goldberg

Project M720-5
U. S. Navy Department, Office of Naval Research
Contract N6-onr-232, Task Order No. V
October 31, 1947

QUARTERLY PROGRESS REPORT

INTRODUCTION

To predict or calculate the profile of a blended line in the ultraviolet spectrum the following procedure is indicated. From a multiplet table including all elements known to give strong lines in the ultraviolet region the components of the blended lines must be found. The relative strengths of the lines must be considered in making identifications.

The intensity of a given line of a given element is determined, first by the abundance of the element in the solar atmosphere, second by the number of atoms in a condition to absorb energy of wave length λ , and third by the f -value or the transition probability of the atom for the line in question. The abundance of the solar elements has been fairly well established from studies of line intensities in the visible portion of the spectrum, but may need modification when the ultraviolet and infrared line intensities become available. The population of the various energy states involved depends on the excitation temperature, and a fairly reliable guess can be made for this value. Finally, transition probabilities for the ultraviolet lines are almost completely unknown. Their determination must come from quantum mechanics or from laboratory measures of intensity.

The profile of each line making up the blend must be considered and then combined in an appropriate fashion. This requires both an adequate theory for the transfer of radiation in and out of a line through the solar atmosphere, and a knowledge of the kinetic temperature and pressure of the atmosphere in the regions in which the line is formed. It is with the determination of these latter quantities that this paper is concerned.

The half width of a weak line is directly proportional to the mean square velocity of the atoms or to the square root of the kinetic temperature.

The width of strong lines depends on collisional broadening effects, and therefore on pressure and temperature.

The curve of growth method for determining these quantities is an extremely powerful one, as it evades some of the difficulties of radiation transfer theory which must be used when determining these quantities from the profile of a single line.

SECTION I

In previous studies of the solar curve of growth, the fit between the observed and theoretical curves has been based on the assumption of line formation following the Schuster-Schwarzchild model. The adoption of the Milne-Eddington approximation to line profiles, in place of the S-S model yields theoretical contours in better agreement with the observed contours. For this reason, we adopt the M-E model. Furthermore, as Menzel, Baker and Goldberg¹ have shown, if the opacity of the solar atmosphere varies with wave length, then the number of effective absorbing atoms will exhibit a reciprocal variation. Since the available data for the elements iron, titanium and vanadium cover the wave length range from 3000 Å to 5000 Å, a proper analysis will take into consideration the variable continuous opacity.

The complete expression for the intensity of emergent radiation of wave length λ and direction θ expressed in terms of the adjacent continuous spectrum is²

$$\frac{I_{\lambda}(0, \theta)}{I_{\circ}(\theta)} = (1 + \beta_{\circ} \cos \theta)^{-1} \left\{ 1 + 3\alpha^2 \beta_{\circ} \cos \theta + \frac{1 - 3\alpha^2}{1 + 2\alpha} \cdot \frac{2\alpha\beta_{\circ} - 1}{1 + 3\alpha \cos \theta} \right\}$$

where β_{\circ} = coefficient of limb darkening

$$3\alpha^2 = (1 + s/k)^{-1}$$

s_{λ} = line scattering coefficient at wave length λ

k = the general absorption coefficient

We are neglecting the line absorption coefficient which is generally small in comparison to the line scattering coefficient s_{λ} . This equation has been used to determine the profiles of absorption lines for the sun's center ($\cos \theta = 1.0$)

¹ Ap J. 87, 81, 1958

² Unsöld. Physik der Sternatmosphären, p. 242. (Springer 1938)

where the value of s_{λ} has been taken from the work of Hjerting.³ The equivalent widths were obtained by numerical integration. The results of the calculations are given in Table I. These curves have been computed for

$$a = \frac{\Delta\lambda_N}{\Delta\lambda_D} = 0.0, 0.001, 0.01, \text{ and } \beta_0 = 5, 2.5, 1.0, 0.5$$

where a is the ratio of natural line width to Doppler width and β_0 is the limb darkening coefficient.

The strength of an absorption line is a function of the limb darkening coefficient which varies from about 10 at 3000 Å to 1/2 at 12,000 Å. Its effect can be seen by a simple argument. Since the deeper layers of the atmosphere are at a higher temperature, the peak of the planckian curve is shifted to the violet in accordance with the Wien displacement law and the energy output increases so that in the violet the deeper layers are sending us more energy than the corresponding layers in the red. Hence, in the violet we see deeper into the atmosphere, and therefore experience a greater limb darkening coefficient. In the first approximation, the number of effective absorbers producing a line in the violet is twice that for the red portion of the spectrum.

The data of King⁴ on relative gf values for Fe I, Ti I and V I have been tabulated with the corresponding equivalent widths of the lines determined by Allen.⁵ Equivalent widths for about 50 additional lines have been obtained from the Utrecht Atlas. All lines below 3900 Å were arbitrarily excluded because of blends.

The lines of titanium were grouped according to excitation potential, the range in excitation potential of each group being small. The lines of each group were then plotted in the form of curves of growth. Two procedures were followed. For the first, the abscissa chosen was $\log gf \cdot \lambda$ with ordinate $\log W/\lambda$. A mean curve of growth was then fitted to each group of points and the relative displacements in abscissa determined. Table II, column 2 gives the displacement Y obtained for each mean excitation potential. A weighted least squares solution of the slope of the resulting straight line gives a temperature of 4495°K for titanium.

³Ap. J. 88, 508, 1938

⁴Ap. J. 87, 40, 1938

⁵Memoirs Commonwealth Solar Observatory, No. 6, 1938

A second plot was made in which corrections for the variable continuous absorption coefficient, as determined by Münch,⁶ and for the limb darkening coefficient, from Table I, were applied to the abscissa. These curves, as obtained for each group of excitation potentials, show a noticeable reduction in the scatter of the points about the mean. The displacements, Y' , are given in Table II, column 3 and are plotted against the group excitation potentials in Figure I. The resulting temperature is $4640^{\circ}\text{K} \pm 290^{\circ}$.

Iron and vanadium were treated in a similar fashion. For iron the excitation temperature is 4770° by the second method. For vanadium, however, the plot of displacement as a function of excitation potential is non-linear and no proper temperature can be found. See Figure 1.

In order to determine the variation of the curve of growth with wave length from the observations, and not from theory, the displacement of each absorption line from the mean curve of growth ($\log gf \cdot \lambda$ vs. $\log W/\lambda$) was obtained for each group and plotted as a function of wave length. The resulting curve is shown in Figure 2. The agreement with the predicted curve, represented by the dotted line, shows that the observations contain no further wave length dependence other than the two assumed in the theory.

For the elements iron and titanium, the groups, corrected for wave length dependences, were brought into their respective curves of growth by use of the weighted excitation temperature 4680°K . The vanadium groups were brought to a mean curve of growth by empirically correcting the smooth line through the points (see Figure 1) to a horizontal line. The mean curves of growth for each element were then assembled into a master curve by sliding them horizontally until the best fit was obtained. The final curve is shown in Figure 3. The solid line represents the mean curve through the observations. A comparison of the theoretical curve computed for the sun's center by the M-E model, ($\beta_0 = 2.5$, $a = 0.01$, dotted line of Figure 3), with the observational curve shows considerable disagreement. The best fit for the Doppler portion is obtained when $\log W/2\Delta\lambda_D = 0.0$, and $\log W \cdot 10^6/\lambda = 1.225$. The corresponding kinetic temperature is $19,500^{\circ}\text{K}$ with an estimated error of $\pm 4000^{\circ}\text{K}$. The fit of the theoretical curve with the observed curve is very poor in the damping

⁶Ap. J. 102, 385, 1945

portion. For lines on the beginning of the square root portion, $a \approx 0.01$; for the strongest iron lines, $a \approx 0.05$, as compared to the classical value of 0.003.

The large Doppler width of the lines as obtained from the curve of growth can be interpreted as due to a high kinetic temperature or to a "normal" temperature of 5700°K plus widening due to relatively small scale turbulence. The formulae for the two cases are

$$(A) \quad \frac{\Delta\lambda}{\lambda} = \frac{1.66}{c} \sqrt{\frac{2kT_1}{\mu}} \quad \text{temperature alone}$$

$$(B) \quad \frac{\Delta\lambda}{\lambda} = \frac{1.66}{c} \sqrt{\frac{2kT_2}{\mu} + v_t^2} \quad \text{temperature and turbulence.}$$

These formulae fit the observations for iron (atomic weight 56) when $T_1 \approx 20,000^\circ\text{K}$, or $T_2 = 5700^\circ$ and $v_t = 2.00 \text{ km/sec}$.

The half widths of faint lines of the elements Ni₅₈, Fe₅₆, Cr₅₂, V₅₁, Si₂₈, Al₂₇, Na₂₃, O₁₆, and lines tentatively identified as C₁₂ have been obtained from the Utrecht Photometric Atlas of the sun. Corrections for instrumental profile and variations in central intensity were applied. The results are in good agreement with formula (A) with a temperature of 16,000°K. See Figure 4.

The observational curve of growth as determined by K. O. Wright from the same data, but without the corrections for variable opacity and limb darkening coefficient, is in good agreement with our curve, but on the average it is slightly below our mean curve. Table III gives the comparison. In this table we also include the data of P. Rubenstein. She has determined her curve from Allen's data, and the theoretical values of $\log X_0$. Her curve is limited in the range of values and lies considerably below ours, which accounts for the low value of temperature that she obtains, $5400^\circ \pm 1300^\circ \text{ m.e.}$

Interpreting Wright's curve on the basis of temperature alone, a turbulent velocity of 0.9 km/sec and a kinetic velocity of 1.3 km/sec correspond to 1.58 km/sec or 8000°K. His value of the damping constant $\Gamma/\nu = 2.61 \times 10^{-6}$ corresponds to $a = .04$, where "a" is the ratio of natural line width to Doppler width as defined by Mitchell and Zemansky.

The large difference in temperature between Wright's results and ours is explained partly by the slight difference in the observational curves, which accounts for 3000° , but mainly by the great difference in the theoretical curves of growth as computed on the S-S model and the M-E model. The latter gives much shallower lines. The central intensity is proportional to the square root of the line absorption coefficient, whereas the S-S model gives intensities proportional to the line absorption coefficient. In Table IV we give the calculated curves of growth.

SECTION II

The partition function $\sum_{s=0}^{\infty} g_{rs} e^{-\frac{\chi_{rs}}{kt}}$ has been computed for Mn I, Mn II, Rh I, Ni I, Pd I, Co I, Cr I, Cr II, Zr I, Zr II, Ce II, Fe I, Ti I, Ti II, and Rn I. A temperature of 5040°K was used. The list of elements was governed by the identified lines in the region $\lambda\lambda$ 3430-3445 which was selected as one suitable for trial predictions of the spectrum. This region is not too complex and covers portions of the spectrum where the continuous background seems to be high or normal, and also portions in which the background is considerably depressed from overlapping lines.

TABLE I

Theoretical Curves of Growth

Based on the Milne-Eddington Model

Log s/k	a = 0.0, $\beta_0 =$				a = 0.001, $\beta_0 =$				a = 0.01, $\beta_0 =$			
	0.5	1.0	2.5	5.0	0.5	1.0	2.5	5.0	0.5	1.0	2.5	5.0
-2.0	-2.52	-2.34	-2.22	-2.09	-2.52	-2.37	-2.22	-2.15	-2.52	-2.37	-2.22	-2.18
1.5	2.02	1.84	1.72	1.59	2.02	1.87	1.72	1.65	2.02	1.87	1.72	1.68
1.0	1.54	1.36	1.24	1.11	1.54	1.39	1.24	1.17	1.54	1.39	1.24	1.20
-0.5	1.06	0.91	0.79	0.67	1.06	0.94	0.79	0.76	1.06	0.94	0.79	0.75
0.0	0.63	0.51	0.42	0.29	0.64	0.52	0.42	0.37	0.63	0.52	0.41	0.37
+0.5	0.33	0.22	-0.15	-0.01	0.32	0.23	-0.14	-0.11	0.32	0.25	-0.13	-0.10
1.0	-0.10	-0.03	+0.04	+0.16	-0.11	-0.04	+0.04	+0.10	-0.09	-0.02	+0.05	+0.09
1.5	+0.07	+0.10	0.18	0.27	+0.06	+0.12	0.18	0.22	+0.08	+0.11	0.18	0.21
2.0	0.17	0.20	0.26	0.36	0.17	0.22	0.26	0.31	0.20	0.24	0.30	0.31
2.5	0.26	0.28	0.32	0.42	0.26	0.30	0.33	0.38	0.33	0.35	0.42	0.42
3.0	0.32	0.34	0.37	0.47	0.34	0.36	0.39	0.44	0.46	0.50	0.56	0.58
3.5	0.38	0.38	0.42	0.51	0.42	0.45	0.48	0.54	0.61	0.68	0.75	0.78
4.0	0.42	0.43	0.45	0.55	0.53	0.57	0.62	0.67	0.82	0.89	0.97	1.00
4.5	0.44	0.46	0.49	0.58	0.68	0.73	0.79	0.84	1.04	1.12	1.21	1.24
5.0	0.45	0.49	0.51	0.60	0.84	0.91	0.98	1.04	1.29	1.37	1.46	1.49
5.5	0.46	0.51	0.54	0.61	1.05	1.13	1.22	1.27	1.54	1.61	1.70	1.73
+6.0	+0.48	+0.53	+0.56	+0.63	+1.27	+1.36	+1.46	+1.53	+1.79	+1.87	+1.96	+1.99

TABLE II

Displacements of Individual Curves of Growth
for Groups of Different Excitation Potential

Element	E_p	Y	Y'
Titanium	0.022	4.48	4.61
	0.832	5.43	5.51
	1.051	5.59	5.72
	1.441	6.17	6.20
	1.736	6.26	6.42
	1.871	6.55	6.59
	2.258	7.13	7.16
Iron	0.059	4.40	4.92
	0.942	5.61	5.61
	1.535	6.17	6.48
Vanadium	0.032	6.00	6.15
	0.279	6.05	6.22
	1.055	6.93	7.04
	1.407	6.93	6.94
	1.370	6.74	6.94
	1.857	7.70	7.98
	1.926	7.96	7.83
	2.088	7.86	8.06
	2.353	8.54	8.62
2.670	10.12	10.24	

TABLE III

Comparison of Observational Curves of Growth

Log X_0	Log W/λ			Differences	
	Rubenstein	Wright	Pierce-Boutelle	R - P-B	W - P-B
-2.0	-----	-7.05	-7.05	-----	.00
-1.5	-----	-6.55	-6.55	-----	.00
-1.0	-5.93	-6.06	-6.03	+.10	-.03
-0.5	-5.54	-5.57	-5.53	-.01	-.04
0.0	-5.23	-5.15	-5.12	-.11	-.03
+0.5	-4.99	-4.88	-4.88	-.11	.00
+1.0	-4.84	-4.75	-4.72	-.12	-.03
+1.5	-4.73	-4.66	-4.60	-.13	-.06
+2.0	-4.59	-4.54	-4.49	-.10	-.05
+2.5	-4.43	-4.35	-4.32	-.11	-.03
+3.0	-4.14	-4.12	-4.16	+.02	+.04

TABLE IV

Comparison of Calculated Curves of Growth

Log s/k	Log W/2Δλ _D		S-S - M-E
	S-S Model Baker's Formula a = 0.04	M-E Model β ₀ = 2.5 a = 0.01	
-2.0	-2.06	-2.05	-.01
-1.5	-1.56	-1.56	.00
-1.0	-1.08	-1.07	-.01
-0.5	-0.63	-0.63	.00
0.0	-0.24	-0.28	+.04
+0.5	+0.05	-0.06	+.11
+1.0	+0.24	+0.10	+.14
+1.5	+0.36	+0.23	+.13
+2.0	+0.49	+0.34	+.15
+2.5	+0.67	+0.42	+.25
+3.0	+0.89	+0.63	+.26
+3.5	+1.13	+0.84	+.29
+4.0	+1.38	+1.06	+.32
+4.5	+1.62	+1.31	+.31
+5.0	+1.87	+1.56	+.31
+5.5	-----	+1.82	-----
+6.0	-----	+2.08	-----

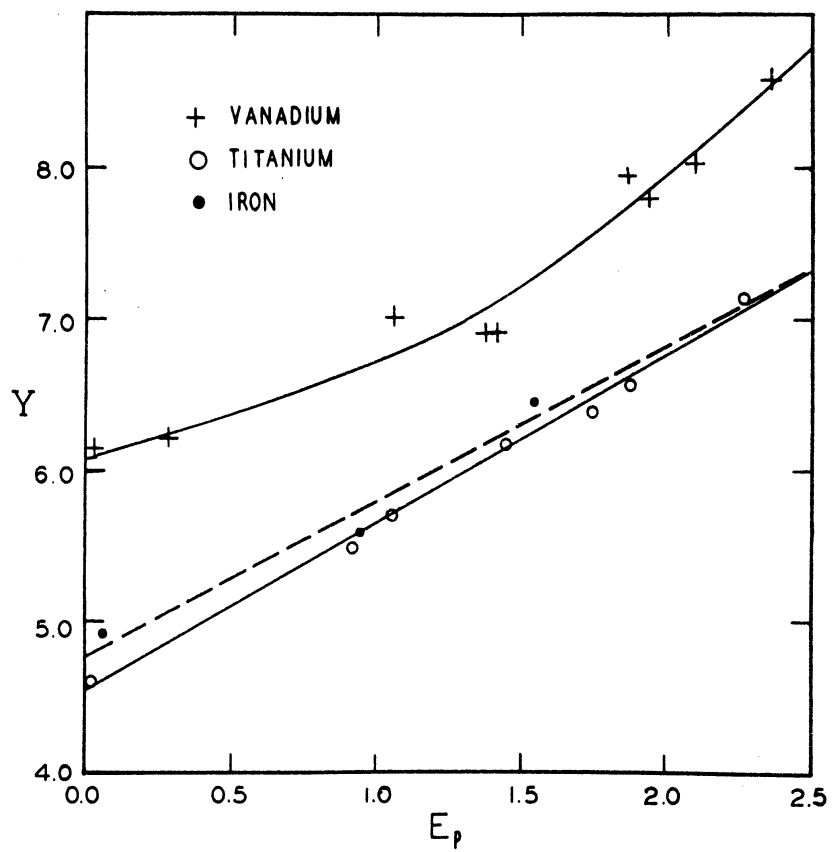


FIG. 1

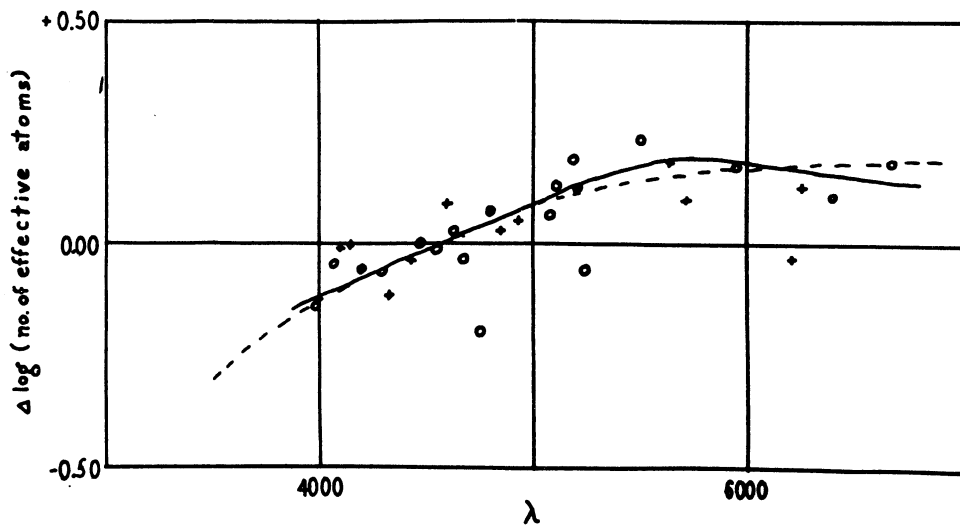


FIG. 2

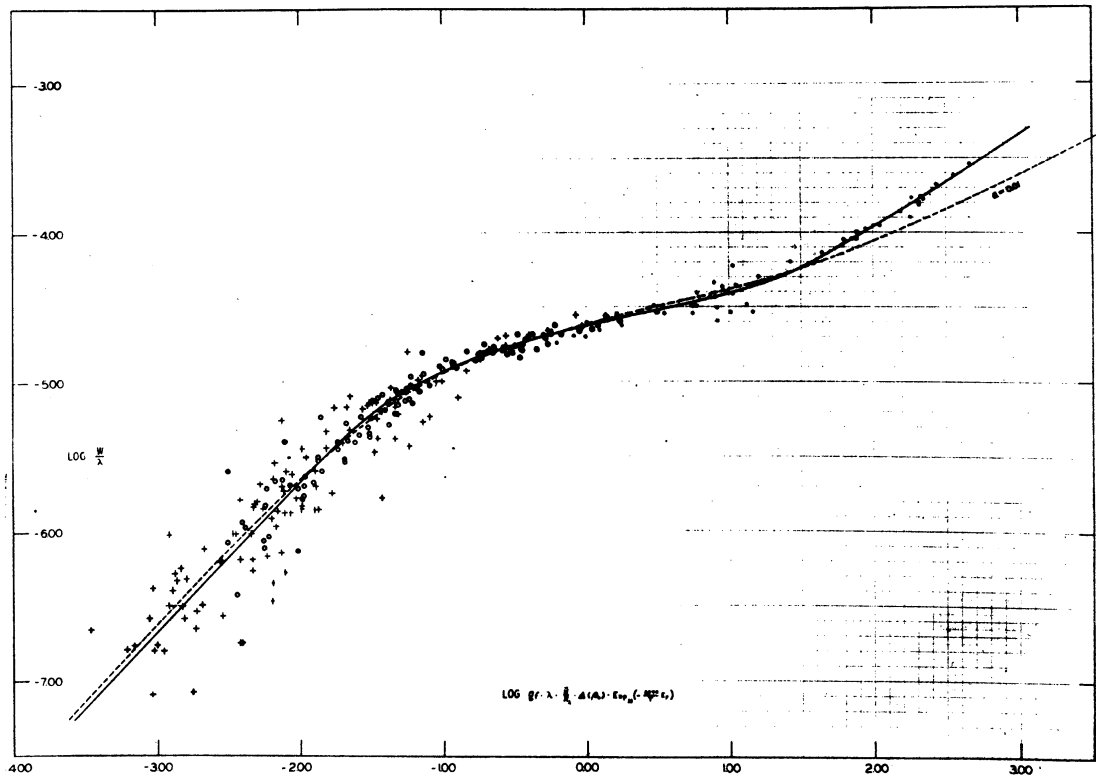


FIG. 3

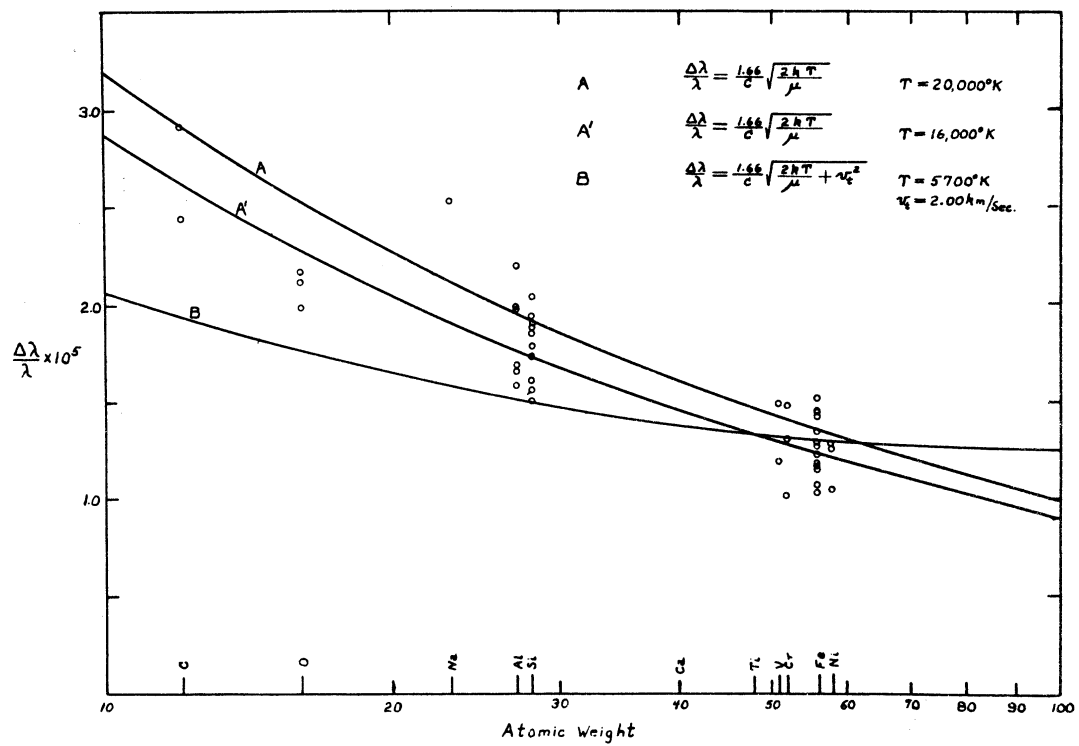


FIG. 4

